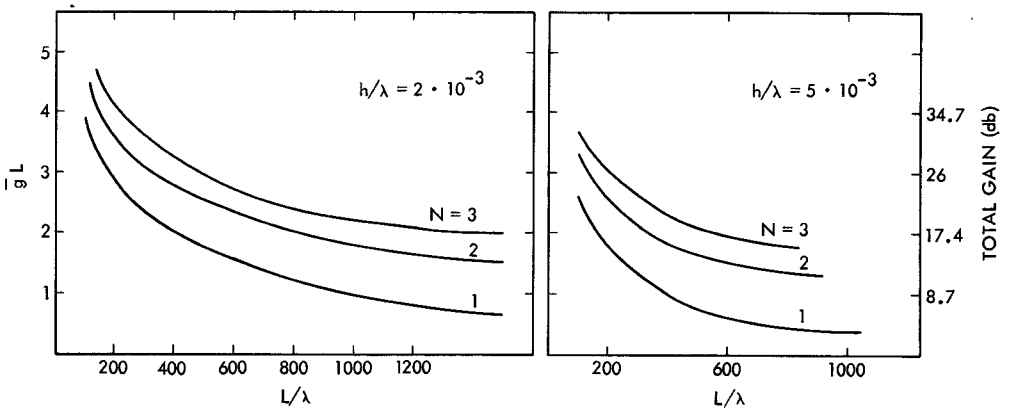

Fig. 3. Oscillation threshold average gain coefficient as a function of L/λ. N corresponds to the longitudinal modes.

For the purpose of this letter, we are only interested in evaluating the order of magnitude of X. McGarr and Alsop [8] have determined analytically and experimentally the reflection from vertical boundaries, and they have shown that both r_1 and r_2 are of the same order of magnitude as h/λ, and that r_2 is many times larger than r_1 (and both are negative for $h \ll \lambda$). Thus we can say that:

$$X \sim ih/\lambda^2 \tag{3}$$

or in a normalized form:

$$XL \sim ihL/\lambda^2 \tag{4}$$

where L is the length of the grating.

III. THRESHOLD OSCILLATION GAIN

Kogelnik and Shank [4] have derived the relation between the coupling coefficient XL, the threshold gain coefficient g, and the wave vector mismatch $\delta(\delta = \beta - \beta_0 =$ difference between the operating wave vector and the Bragg wave vector $2\pi/\Lambda)$. Elachi *et al.* [6] generalized their results to the case where there is gain g_1 in the forward direction, and a different gain or loss g_2 in the backward direction. This relation is

$$XL = \pm\psi/\sinh(\psi L) \tag{5}$$

$$\psi = [(\bar{g} - j\delta)^2 - X^2]^{1/2}$$

where

$$\bar{g} = (g_1 + g_2)/2.$$

Equation (5) has many solutions which correspond to the longitudinal spectrum of distributed oscillators [4]. In Fig. 3, we plotted the average gain $\bar{g}$ required for oscillation as a function of L/λ for two values of h/Λ and for different longitudinal modes N. $N = 1$ is the mode nearest to the Bragg frequency. The normalized coupling coefficient was taken as equal to ihL/λ^2.

To illustrate let us consider the case where $\lambda = 3\ \mu$, $\Lambda = 1.5\ \mu$, and $L = 2$ mm. For $h/\Lambda = 4 \times 10^{-3}$, the average gain coefficient needed for the first mode is $\bar{g} = 15\ \text{cm}^{-1}$. For $h/\Lambda = 10^{-2}$, then $\bar{g} = 6\ \text{cm}^{-1}$. These correspond to an average relative imaginary wave vector β_i/β_r equal to 0.75×10^{-3} and 0.3×10^{-3}, respectively. The forward gain g should be well above these values (at least by a factor of 2) to account for the losses due to bulk wave radiations [9], [10] which usually are small, and for the fact that the backward wave is attenuated.

Bers and Burke [11], and Bers [12] have studied in detail the resonant amplification of surface acoustic waves with electrons drifting across a magnetic field with and without diffusion. Referring to their analysis and results it is clear that relative imaginary wave vectors well above 1.5×10^{-3} can be achieved. To minimize the attenuation of the backward wave, the electron drift velocity v_0 should not exceed by far the acoustic wave velocity v_a because otherwise backward resonant attenuation would occur at about the same frequency as forward resonant amplification.

Taking $v_0/v_a = 5$, β_i/β_r is larger than 1.5×10^{-3} over a very wide frequency band from about $\simeq 10^{-3}\omega_\sigma$–$\sim 0.1\omega_\sigma$ depending on the magnetic field and the diffusion coefficient. ω_σ is the effective carrier relaxation frequency [11], [12].

IV. CONCLUSION

Even though the preceding study is approximate, it is clear that DFB oscillation can be achieved in surface acoustic wave amplifiers. Surface corrugations with periods as short as 0.1 μ have recently developed using holographic techniques [13]. Thus ultrahigh frequency oscillators could be developed if semiconductors with high enough relaxation frequency, and low-diffusion coeficients are available.

REFERENCES

[1] H. Kogelnik and C. V. Shank, *Appl. Phys. Lett.*, vol. 18, p. 153, 1971.
[2] K. O. Hill and A. Watanabe, *Opt. Commun.*, vol. 5, p. 389, 1972.
[3] D. P. Schnike, R. G Smith, E. G. Spencer, and M. F. Gavin, *Appl. Phys. Lett*, vol. 21, p. 494, 1972.
[4] H. Kogelnik and C. V. Shank, *J. Appl. Phys.*, vol. 43, p. 2327, 1972.
[5] C. Elachi and C. Yeh, *J. Appl. Phys.*, vol. 7, p. 3146, 1973.
[6] C. Elachi, G. Evans, and C. Yeh, presented at the Integrated Optics Conf. (New Orleans, La.), Jan. 1974.
[7] W. S. C. Chang, "Periodic structures and their application in integrated optics," *IEEE Trans. Microwave Theory Tech. (1973 Symposium Issue)*, vol. MTT-21, pp. 775–785, Nov. 1973.
[8] A. McGarr and L. E. Alsop, *J. Geophys. Res.*, vol. 72, p. 2169, 1967.
[9] H. S. Tuan and C. P. Chang, "Tapping of Love waves in an isotropic surface waveguide by surface-to-bulk wave transduction," *IEEE Trans. Microwave Theory Tech.*, vol. MTT-20, pp. 472–477, July 1972.
[10] H. L. Bertoni, "Piezoelectric Rayleigh wave excitation by bulk wave scattering," *IEEE Trans. Microwave Theory Tech. (Special Issue on Microwave Acoustics)*, vol. MTT-17, pp. 873–882, Nov. 1969.
[11] A. Bers and B. E. Burke, *Appl. Phys. Lett.*, vol. 16, p. 300, 1970.
[12] A. Bers, in *Proc. IEEE 1970 Ultrasonics Symposium*, Oct. 1970.
[13] C. V. Shank and R. V. Schmidt, *Appl. Phys. Lett.*, vol. 23, p. 156, 1973.

Surface Acoustic Wave UHF Interferometer

GENE CHAO AND LOUIS BREETZ

***Abstract*—A 330-MHz surface acoustic wave (SAW) interferometer is described. The delay for the interferometer is provided by a 6.67-μs ST quartz SAW delay line. The interferometer is capable of 50-dB nulls of 150-kHz periodicity over a 10-MHz instantaneous bandwidth.**

Manuscript received March 11, 1974; revised June 10, 1974.
The authors are with the Naval Research Laboratory, Washington, D. C. 20375.

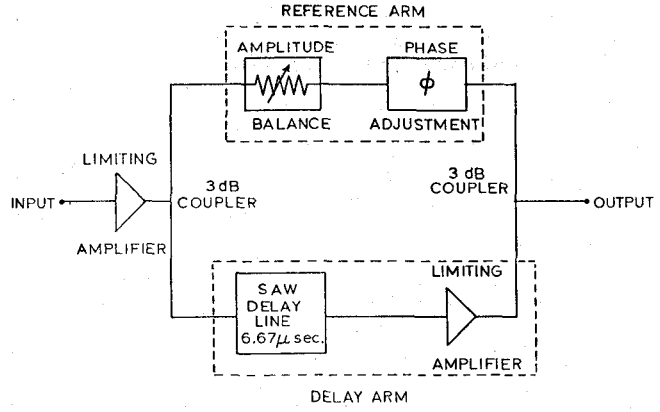

Fig. 1. Schematic of SAW interferometer circuit. For input signal $A_1 \exp(j\omega t)$, output signal is $A_2[1 + \exp(-j\omega\tau] \exp(j\omega t)$, where τ is the time delay of the SAW delay line.

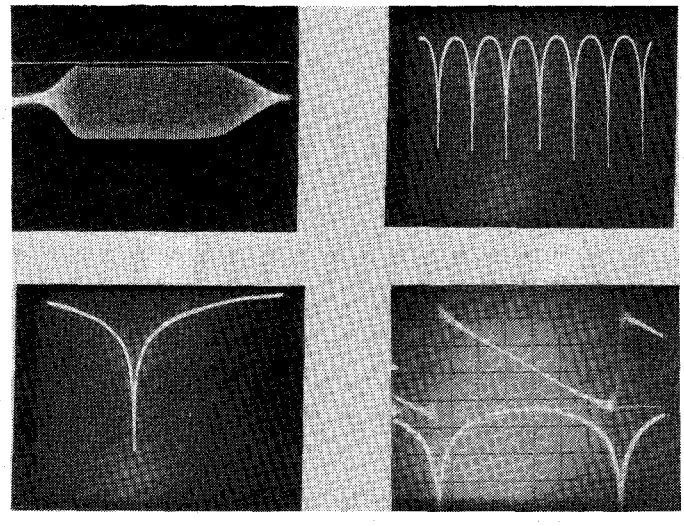

Fig. 2. Response of SAW interferometer circuit. (a) Linear amplitude versus frequency: ordinate is relative amplitude, abscissa is 2.0 MHz/division, f_0 = 330 MHz. (b) Logarithmic amplitude versus frequency: ordinate is 10 dB/division, abscissa is 100 kHz/division, the sweep time of 10 s/division was still too fast to record actual nulls. (c) As in (b): ordinate is 10 dB/division, abscissa is 10 kHz/division, sweep time is 10 s/division. (d) Amplitude, lower trace, [and phase, upper trace] versus frequency: ordinate is 10 dB/division [and 45°/division], abscissa is f_0 = 333.880 MHz ± 112 kHz. Nulls are 150 kHz apart.

The Federal Communications Commission has allocated portions of the UHF band to the Federal Aviation Administration for use as airline glide-path (g-p) signals. These signals fall between 329.15 and 335.00 MHz with 150-kHz periodicity, and can interfere with communications systems operating in close proximity to airports. The purpose of this letter is to describe a method of nulling these signals.

It is well known that surface acoustic wave (SAW) delay lines provide time delays some five orders of magnitude larger than electromagnetic waves for the same physical length. In addition, they suffer less loss per wavelength below 2 GHz. Several authors have described SAW devices which make use of these properties for highly selective bandpass filters and frequency discriminators [1]–[3]. In this work we use a 6.67-μs SAW delay line in an interferometer circuit to produce a series of periodic nulls 150 kHz apart. The SAW delay line is made of 35 pairs of interdigital fingers placed at each end of an ST quartz substrate. The fingers and interspaces are each 2.3 μm wide. The basic circuit is shown in Fig. 1; it consists of a simple interferometer circuit with a SAW delay line and amplitude and phase controls to adjust the location and depth of the interference nulls. The output consists of two signals of equal amplitude with the phase of one varying as $w\tau$ {output = $A_2[1 + \exp(-j\omega\tau)] \exp(j\omega t)$}. The transfer function of the device is of the form $A \exp(-j\omega\tau/2) \cos(\omega\tau/2)$, where $\exp(-j\omega\tau/2)$ is a delay term and $\cos(\omega\tau/2)$ gives the null information where the null spacing is $1/\tau = \Delta f$. The limiting amplifier following the SAW delay line is used to flatten the amplitude response through the delayed arm in order to achieve deep interference nulls over the entire band of interest. This was especially necessary since we used a simple SAW delay line having a $[(\sin x)/x]^2$ frequency response [4]. A further refinement would be to use a SAW rectangular bandpass filter [5].

The response of the circuit is shown in Fig. 2. In addition to flattening the response, the amplifier compensates for the 25-dB delay line loss. Fig. 2(a) is a linear amplitude versus frequency sweep showing some 65 nulls between 325 and 335 MHz. Fig. 2(b) and (c) is logarithmic amplitude versus frequency expanded views of the null train. It was observed that even for the case of Fig. 2(b), the frequency sweep was too fast for the spectrum analyzer to record the actual values of the nulls. In Fig. 2(c), a 65-dB null is shown.

In a sample of 13 consecutive nulls, the deepest was 65 dB, the shallowest 49 dB, and the mean 57.5 dB. If any one null is optimized, better than 70 dB is achieved. It should be noted that a 50-dB null

implies an unbalance of only 0.027 dB between the reference and delayed arms of the interferometer, indicating that some type of limiting may be necessary even if a SAW bandpass filter is used. Fig. 2(d) is an oscillogram of the amplitude and phase characteristics of the interferometer. The phase is very linear, running from +90° to −90° between each null.

In summary, the SAW interferometer described is capable of 50-dB nulls of 150-kHz periodicity over frequency bands limited by the SAW transducers used. The limiting amplifier provides the dual benefit of ultraflat frequency response using standard $[(\sin x)/x]^2$ transducers and enough gain to compensate for delay line losses. Because the nulls are extremely narrow and deep, most of the UHF band involved remains available for use in communications systems. When a satellite navigation system receiving station is unavoidably in the presence of the g-p transmission field, its highly sensitive receiver can easily be blocked so that it would be insensitive to the low level CW (with Doppler shift) received from a distant satellite. Each allocated 150-kHz-spaced g-p signal with its narrowly spaced sidebands falls well within a deep rejection notch. The frequencies of the satellite CW signals happen to fall sufficiently outside these notches to be received at an acceptable useful level.

REFERENCES

[1] P. Hartemann, "Narrow-bandwidth Rayleigh-wave filters," *Electron. Lett.*, vol. 7, pp. 674–675, Nov. 1971.
[2] P. Hartemann and O. Menager, "Rayleigh-wave discriminator," *Electron. Lett.*, vol. 8, pp. 214–215, Apr. 1972.
[3] A. J. Budreau and P. H. Carr, "Narrow-band surface wave filters at 1 GHz," in *Proc. 1972 IEEE Conf. Ultrasonics*, 1972, pp. 218–220.
[4] W. R. Smith *et al.*, "Analysis of interdigital surface wave transducers by use of an equivalent circuit model," *IEEE Trans. Microwave Theory Tech. (Special Issue on Microwave Acoustics)*, vol. MTT-17, pp. 856–864, Nov. 1969.
[5] C. S. Hartmann, D. T. Bell, Jr., and R. C. Rosenfeld, "Impulse model design of acoustic surface-wave filters," *IEEE Trans. Sonics Ultrason. (Special Issue on Microwave Acoustic Signal Processing)*, vol. SU-20, pp. 80–93, Apr. 1973.

An Accurate Formula for the Gamma Function

L. LEWIN

***Abstract*—The residue calculus method of investigation of certain waveguide configurations makes use of the asymptotic properties of the gamma function. Usually the range of the variables concerned is such that this approximation is quite adequate. In a recent investigation of a very narrow waveguide junction peculiar numerical effects were traced to a condition where the variables were much too small to warrant the use of the usual asymptotic formula. A new and very simple modification extends the asymptotic form right down to zero with an error of, at most, only a few percent.**

Manuscript received May 20, 1974.
The author is with the Department of Electrical Engineering, University of Colorado, Boulder, Colo. 80302.

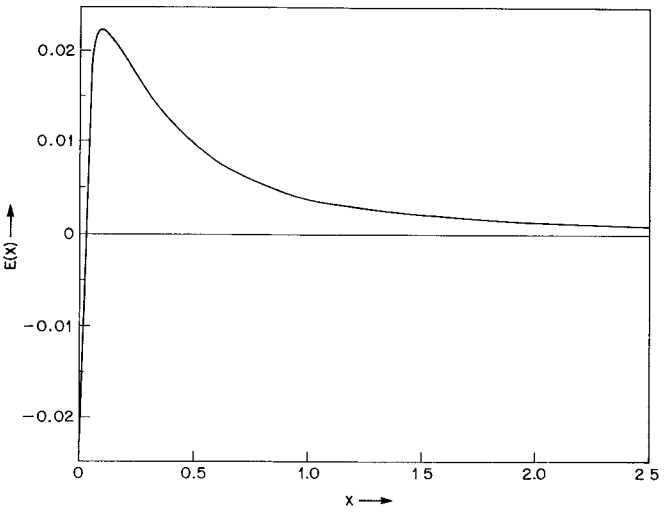

Fig. 1.

In the course of a recent investigation by the residue-calculus method of a waveguide junction with a very large dimensional ratio, it was noticed that the numerical values of some of the coefficients in the calculation were behaving quite differently from what was expected. The matter was eventually traced to an inappropriate use of the asymptotic formula for the Γ function. This is usually given in the form, valid for large x,

$$\log \Gamma(x) = (x - \tfrac{1}{2}) \log x - x + \tfrac{1}{2} \log (2\pi) + \left\{ \frac{1}{12x} - \frac{1}{360x^3} + \cdots \right\}. \quad (1)$$

In the example the values of x to be used included some close to zero, and although the correction series in $1/x$ in (1) is not usually utilized in these formulas it is clear that, even in truncated form, (1) is useless so close to the origin. The departure from the anticipated values is therefore to be expected.

In the course of working out these features an amended formula for the Γ function was found. Although it only involves a simple derivation from (1), it appears to be new, and is offered here in case it has a wider use than the particular problem that gave rise to it. It comes from incorporating the $1/12x$ term with $1/2 \log x$ (somewhat after the manner of Padé approximations), and can be written

$$\log \Gamma(x) = (x - 1) \log x - x + \tfrac{1}{2} \log (2\pi) + \tfrac{1}{2} \log (x + \tfrac{1}{6}) + E(x). \quad (2)$$

Here, $E(x)$ is a correction term which is quite small for all positive values of x, and can usually be neglected. For large x it is closely approximated by $(12x + 46/15)^{-2}$, but even for values right down to $x = 0$ it remains sufficiently small to enable the dominant terms in (2) to represent $\Gamma(x)$ to within about 2 percent. A graph of $E(x)$ from $x = 0$ to 2.5 is shown in Fig. 1.